

Response to Anonymous Referee #1

We would like to sincerely thank Referee #1 for their time in reviewing this manuscript and for their positive feedback. We found the provided comments and suggestions very constructive for improving this paper. Our responses to each comment are provided below in black fonts and the Referee's comments are indicated in blue fonts. All the mentioned line and section numbers refer to the originally submitted manuscript unless stated otherwise.

Major Comments:

Model Architecture and Process Representation

The manuscript would benefit from:

- A more comprehensive comparison of core model mechanisms
- Clear explanation of how each model transforms inputs into biogenic flux outputs
- Detailed coverage of key process differences, particularly:
 - GPP calculations from radiation and vegetation parameters
 - Soil moisture influences on photosynthesis and respiration
 - Temperature effects on respiration
 - Phenology implementation approaches

We agree that a more detailed and comprehensive description of the models would help the readers understand better their differences and would promote a better interpretation and discussion of the results. We have followed the Referee's suggestions and we have included process flow diagrams for each model and a Table that summarizes the key equations used by each model for the calculation of GPP, R_{eco} and phenology. We have added this new information in a new Appendix and we have updated Section 2.3 (Model description) with more details, explaining better the different methodological approaches followed by each model, referring to the new information supplied in the Appendix. Additionally, we added four Tables in a Supplement document, which provide the description and the values of the parameters used by each model in this paper. These Tables complement the information provided in the new Appendix, facilitating the understanding of the different model approaches and their parametrisation in this paper.

Below you can find the new text added in Section 2.3 (model description):

diFUME: "GPP is modelled for the vegetation voxels of each horizontal layer (i) based on the PAR reaching the sunlit and the shaded fraction of LAI in each voxel using a nonrectangular hyperbolic function and other empirical functions for the simulation of air temperature, vapour pressure deficit and soil water content effects. R_{eco} is separated into the aboveground and belowground components; the aboveground is modelled based on an exponential fixed- Q_{10} equation using air temperature, multiplied by LAI, and the belowground based on a modified Arrhenius equation using soil temperature and soil water content. The main equations used by diFUME model, as well as a model flow diagram are presented in Appendix A."

JSBACH: "The carbon assimilation is described by the biochemical photosynthesis model of Farquhar et al. (1980). The assimilation rate is limited either by the carboxylation rate ($J_{C,stress}$) or the electron transport rate ($J_{E,stress}$) (Table A1). $J_{C,stress}$ is a function of the maximum carboxylation rate (V_{max}), which has an Arrhenius-type temperature dependence and $J_{E,stress}$ is a function of PAR (non-rectangular hyperbolic dependence) and J_{max} (maximum electron transport rate), which has a linear dependence on temperature. Both V_{max} and J_{max} are inhibited above 55 °C. V_{max} is also scaled with a factor depending on the canopy depth to account for the Rubisco profile in the canopy. Dark respiration (r_d) is a fixed fraction of V_{max} at 25 °C with an Arrhenius-type temperature dependence. It is inhibited above 55 °C and decreased with increasing solar irradiance. The unstressed stomatal conductance ($g_L^{H_2O}$) is scaled by the plant available soil water (f_{ws}) to obtain stomatal conductance under water stress ($g_{L,stress}^{H_2O}$), which is used to derive $J_{C,stress}$ and $J_{E,stress}$ and then finally the assimilation rate under water stress (A_{stress}). f_{ws} depends on soil moisture in the root zone and specific

humidity. The seasonal development of LAI is described by the Logistic Growth Phenology (LoGro-P) model (Böttcher et al., 2016). The development of LAI of broadleaved deciduous trees is described by the summer green phenology (Table A1). It has three phases, the growth period in the spring ($k > 0$ and $p = 0$), the vegetative phase during the summer ($k = 0$ and small p) and the rest phase starting in autumn ($k = 0$ and high p). The transition from the rest phase to the growth phase is dependent on the evolution of the temperature using the alternating model of Murray et al. (1989), while the growth phase has a fixed duration. The maximum LAI is given as a parameter. The grass phenology further includes soil moisture and net primary productivity as determining factors. In the autumn, the phase transition occurs when the pseudo soil temperature (running mean of air temperature) falls below a critical soil temperature, while grasses grow when there is sufficient soil moisture and temperature. Leaves are shed when NPP is negative. The soil hydrology parameters are set on the basis of soil texture. The soil moisture is simulated with five layers within a multilayer soil hydrological scheme. The dynamics of litter and soil carbon is described by the submodel Yasso07 (Tuomi et al., 2009, 2011). Five carbon pools are distinguished based on their chemical properties (acid hydrolyzable, water soluble, ethanol soluble, neither hydrolyzable nor soluble, humus). The first four pools (a,w,e,n) are tracked both above and below ground, and separate pools are used for woody and non-woody litter, altogether 18 pools. The litter pools receive carbon input from vegetation through the litter flux, faeces from grazing and losses from reserve pool (Table A1). Decomposition of the litter pools causes carbon to transfer between the pools and to the atmosphere. The loss rates depend on temperature, water availability and type of litter elements.”

SUEWS: “Photosynthetic uptake is calculated using an empirical canopy-level photosynthesis model, where the potential photosynthesis is modified for different environmental factors (Table A1). The same environmental factors are also controlling the surface (stomatal) conductance. The seasonal development of LAI depends on the growing degree days (GDD) and senescence degree days (SDD), which depend on air temperature. The rates of leaf-on and leaf-off and maximum LAI are given as an input. During the leaf-on period, LAI remains relatively stable and responds slowly to stress conditions. In contrast, other environmental factors that regulate surface conductance exhibit more pronounced responses to stress. Soil and vegetation respiration is calculated as simple exponential dependence on air temperature. SUEWS provides a holistic approach on joint energy, water, and CO₂ cycles in urban environments, allowing to account, for example, for the influence of elevated air temperatures on water and CO₂ cycles. The model relies on standard meteorological inputs like wind speed, air temperature, air pressure, precipitation, and short-wave radiation. The forcing air temperature needs to be from above roughness sublayer, so in this study the measured 2 m air temperature is scaled to 35 m using lapse rate of 6.5°C/km. SUEWS is able to calculate 2 m temperature from the forcing temperature (Tang et al. 2021), which is used in the calculations of photosynthesis and soil and vegetation respiration.”

To facilitate this comparison, please include:

- Process flow diagrams for each model
- Comparative table of key equations and methodological approaches

The process flow diagrams of each model and the table of key equations have been added in a new Appendix. The new information is presented below. The Tables with the model parameters are provided in the Supplement file (attached).

Appendix A. Model architecture and process representation

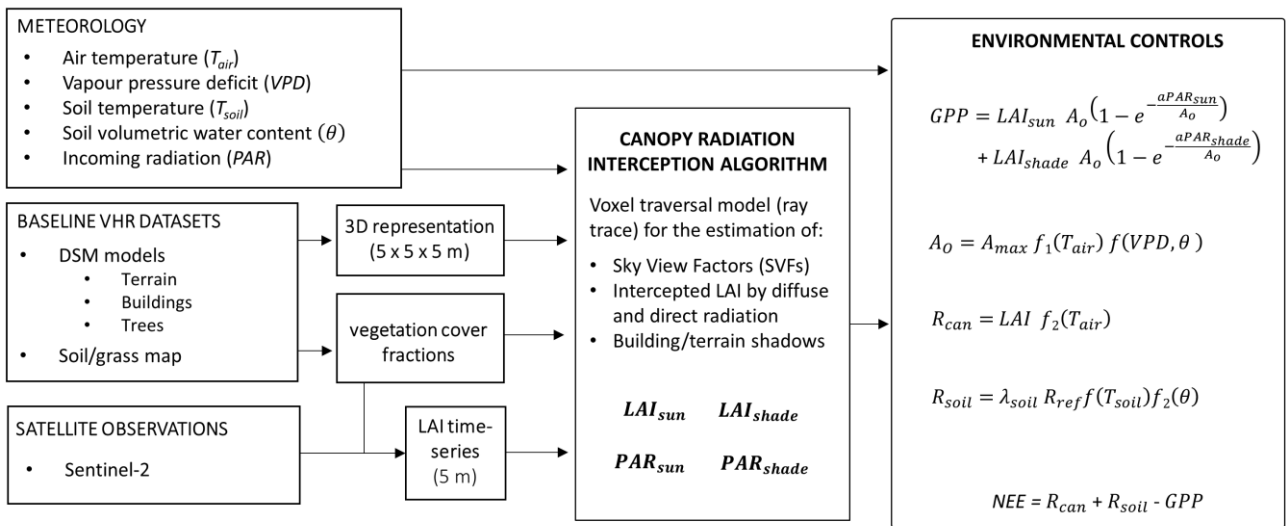


Figure A1. Process flow diagram of the diFUME model. The detailed description of the model can be found in Stagakis et al. (2023a).

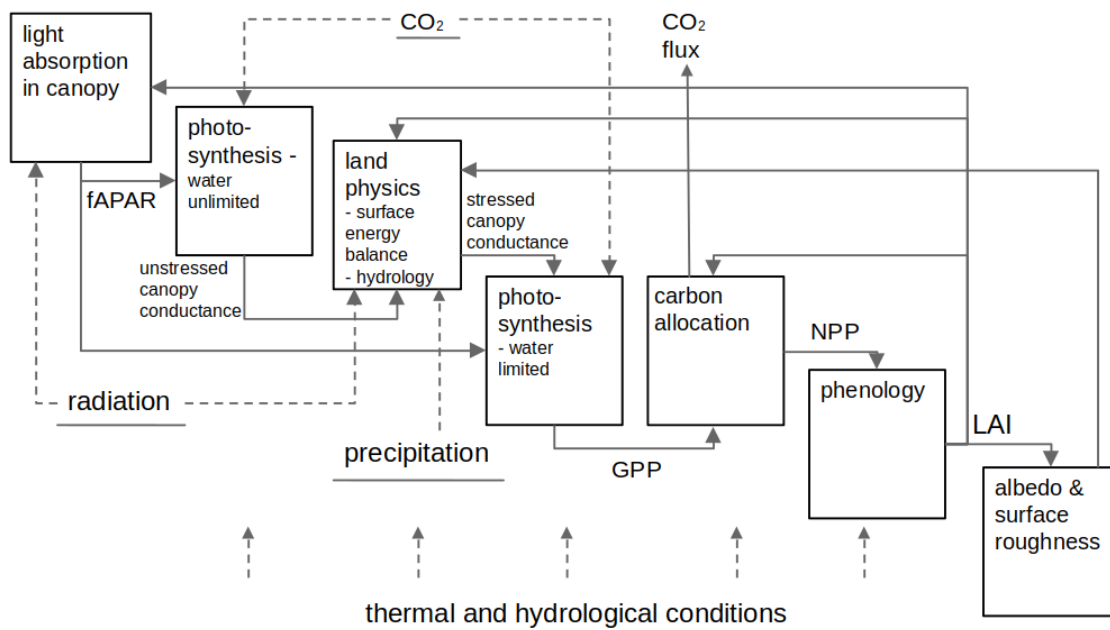


Figure A2. Process flow diagram of the JSBACH model. The detailed description of the model can be found in Reick et al. (2013).

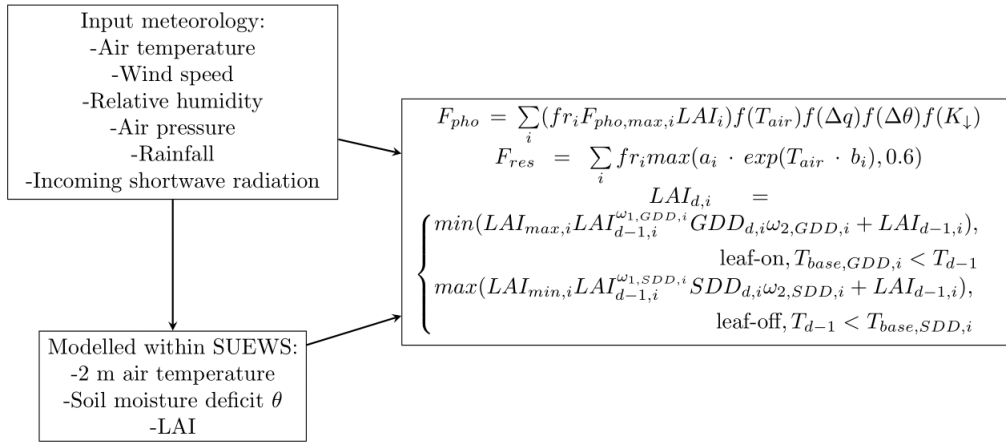


Figure A3. Process flow diagram of the SUEWS model. The detailed description of the model can be found in Järvi et al. (2011, 2019)

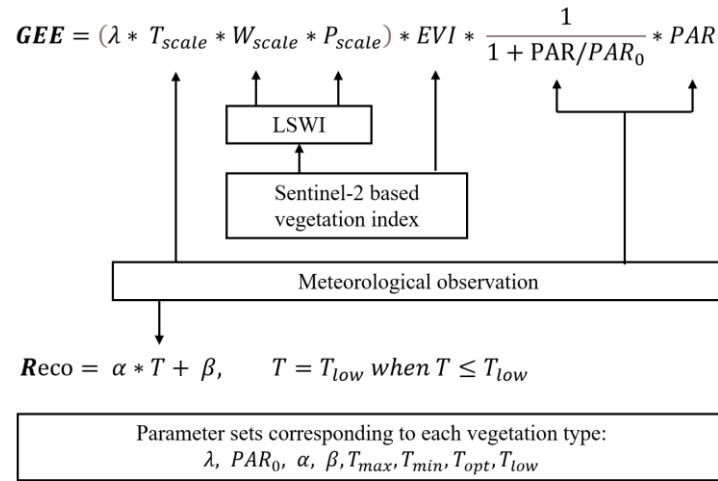


Figure A4. Process flow diagram of the VPRM model. The detailed description of the model can be found in Mahadevan et al. (2008).

Table A1. Overview of the main equations used by each model to estimate gross primary production (GPP), ecosystem respiration (R_{eco}) and phenology. The original notation of each model was preserved to facilitate the comparison with the relevant publications and the flow diagrams. The parameters of the equations are explained in the Supplement. The detailed descriptions of each model can be found in the respective references provided in Section 2.3.

	GPP	R_{eco}	Phenology
diFUME	$GPP = \sum_{i=1}^n \left[\frac{LAI_{sun,i} A_o (1 - \exp(-aPAR_{sun,i}/A_o)) + LAI_{shade,i} A_o (1 - \exp(-aPAR_{shade,i}/A_o))}{A_o} \right]$ $A_o = A_{max} \cdot f(T_{air}) f(VPD, \theta)$ $f(T_{air}) = \exp \left[- (T_{air} - T_{opt})^2 / 2W^2 \right]$ $f(VPD, \theta) \text{ based on: } g_s = \left(g_o + a_1 \frac{A_{net} f(T_{air})}{(1 + \frac{VPD}{D_o})(c_s - \Gamma)} \right) \left(1 - \frac{(\theta_{ref} - \theta)^{b_1}}{(\theta_{ref} - \theta_g)^{b_1}} \right)$	$R_{eco} = LAI D_{sc} R_l + \lambda_{soil} R_{S,ref} \exp \left[E_0 \left(\frac{1}{T_{ref,S} - T_0} - \frac{1}{T_{soil} - T_0} \right) \right] \left[\frac{(\theta - \theta_0)^b}{(\theta_{ref} - \theta_0)^b} \right]$ $R_l = R_{l,ref} Q_{10}^{\frac{T_{air} - T_{ref,l}}{10}}$	<i>LAI derived by Copernicus High Resolution Vegetation Phenology and Productivity (HR-VPP) product</i>
JSBACH	<p><i>Due to the complexity of the full Farquhar et al. (1980) model implementation in JSBACH, only an outline is provided here.</i></p> $GPP = LAI A_{stress}$ $A_{stress} = \min(J_{C,stress}, J_{E,stress}) - r_d$ $g_{L,stress}^{H_2O} = f_{ws} g_L^{H_2O}$	$R_{eco} = R_m + R_g + R_h$ $R_m = LAI r_d / f_{leaf}$ $R_g = (CC - 1) NPP, \text{ when } NPP > 0$ $CC = (NPP + R_g) / NPP$ $R_h = (1 - f_{faeces}) F_{grazing} + k_h C_h + F_{soil}$	$\frac{dLAI}{dt} = kLAI \left(\frac{LAI}{LAI_{max}} \right) - pLAI$
SUEWS	$F_{pho} = \sum_i (fr_i F_{pho,max,i} LAI_i) g(T_{air}) g(\Delta q) g(\Delta \theta) g(K_l)$ $g(T_{air}) = [(T_{air} - T_L)(T_H - T_{air})^{T_c}] / [(G_5 - T_L)(T_H - G_5)^{T_c}]$ $T_c = (T_H - G_5) / (G_5 - T_L)$ $g(\Delta q) = G_3 + (1 - G_3) G_4^{\Delta q}$ $g(\Delta \theta) = [1 - \exp(G_6(\Delta \theta - \Delta \theta_{WP}))] / [1 - \exp(-G_6 \Delta \theta_{WP})]$ $g(K_l) = [K_l / (G_2 + K_l)] / [K_{l,max} / (G_2 + K_{l,max})]$	$F_{res} = \sum_i fr_i \max(a_i \exp(T_{air} b_i), 0.6)$	$LAI_{d,i} = \begin{cases} \min(LAI_{max,i}, LAI_{d-1,i}^{\omega_{1,GDD,i}} GDD_{d,i} \omega_{2,GDD,i} + LAI_{d-1,i}), \\ \text{leaf-on}, T_{base,GDD,i} < T_{d-1} \\ \max(LAI_{min,i}, LAI_{d-1,i}^{\omega_{1,SDD,i}} SDD_{d,i} \omega_{2,SDD,i} + LAI_{d-1,i}), \\ \text{leaf-off}, T_{d-1} < T_{base,SDD,i} \end{cases}$
VPRM	$GEE = (\lambda T_{scale} W_{scale} P_{scale}) EVI [1 / (1 + PAR / PAR_0)] PAR$ $T_{scale} = (T - T_{min})(T - T_{max}) / [(T - T_{min})(T - T_{max}) - (T - T_{opt})^2]$ $W_{scale} = 1 + LSWI / (1 + LSWI_{max})$ $P_{scale} = (1 + LSWI) / 2$	$Reco = \alpha T + \beta$ $T = T_{low}, \text{ if } T \leq T_{low}$	<i>Sentinel-2 vegetation indices</i>

- Discussion of how process representation differences impact model performance across conditions

We have added a more detailed discussion focusing on how the model differences affected their performance in this study. The new text has been added in Section 4.1, which was already discussing the advantages and disadvantages of the different model types in the original manuscript. The new text is presented below:

“All the models require temperature and radiation inputs. However, VPRM requires the least number of data streams among the models (Table 2). diFUME and VPRM use satellite data to track vegetation phenology (Table A1), making them more suitable for monitoring purposes, especially in urban areas where the vegetation type heterogeneity is so pronounced that it is very difficult to model accurately. As demonstrated also by the current study, these satellite-based models are able to detect changes in leaf area due to phenological shifts or stressful events, such as drought, providing valuable insights into ecosystem responses to environmental change. However, these models are not able to predict future carbon cycling under different climate scenarios or planning strategies, as they rely heavily on observations.

Despite the different levels of sophistication of the four models on simulating GPP, all consider some sort of hyperbolic function to model the response of gross photosynthesis to light and a bell-shaped dependence on air temperature (Table A1). On the other hand, the responses of photosynthesis to vapour pressure deficit and soil water availability are accounted very differently in each model. VPRM uses a very simplistic approximation of drought effects on GPP based on LSWI, diFUME and SUEWS use empirical functions, while JSBACH has the most sophisticated approach to modelling drought effects (Section 2.3, Table A1). The generally good agreement between the models in simulated tree GPP seasonally and diurnally indicates that the simple process approximations were sufficient, possibly due to the lack of intense drought effects on tree GPP in this study based on the sap flow observations (Fig. 3a,b). On the other hand, drought effects on lawn GPP were captured by all models during August 2022, with VPRM showing the most intense drought-induced GPP reductions which were repeated in summer 2023 (Fig. 4a,b). These findings indicate that VPRM is very sensitive to LSWI and EVI indices (Fig. B1b,c), which can drive GPP to excessively low values during dry periods, in contrast to the process-based JSBACH and the empirical functions of diFUME and SUEWS. Unfortunately, we do not have any independent measurements of lawn GPP in this study to evaluate which type of model is closest to the truth.

Even though there are some similarities between the models in the representation of the GPP process, the description of R_{eco} significantly differs in terms of approximations and sophistication. JSBACH is the only model tested that includes carbon pools, which are essential for studying long-term temporal dynamics. This feature allows JSBACH to model the behaviour of soil carbon pools and their changes over extended periods. For instance, if high decomposition rates persist, the decreasing soil carbon pool also decreases heterotrophic emissions, whereas other models tested do not have such feedbacks and use only empirical environmental response functions. diFUME uses a more detailed approach compared to SUEWS and VPRM, separating above and below ground respiration and using T_{air} , T_{soil} , SWC and LAI as proxies, whereas SUEWS and VPRM use an exponential and a linear response function on T_{air} respectively (Table A1). Despite the differences in the representation of R_{eco} , the seasonal and diurnal variabilities were not very different between the four models (Fig. 3c,d, 4c,d) and the differences detected were not clearly related to the level of sophistication but rather to the choice in parametrisation. For example, diFUME tree R_{eco} was higher than the other models because the parameterisation was kept the same for lawn and tree sites. JSBACH showed the best performance in predicting lawn R_{eco} (Fig. 6d) but on the other hand, ecosystem process models such as JSBACH require very detailed input information (e.g. on soil carbon stocks) and are based on full-cycle assumptions that are difficult to meet in highly managed and disturbed urban ecosystems where carbon pools are constantly altered by human interventions (Golubiewski, 2006). Furthermore, process-based models such as JSBACH require a large number of input parameters compared to simple light-use-efficiency models such as VPRM which has, in some cases, been found to outperform process-based models in explaining CO_2 variability (Gourdji et al., 2022).”

SUEWS Configuration Concerns

As a key member of the SUEWS development team, I have specific concerns about the model configuration:

1. Forcing Data Level

- Current: Near-surface measurements (2m) used to force SUEWS
- Required: Forcing data from above roughness sublayer (3-5x mean roughness element height)
- Impact: 2m measurements are inappropriate for this purpose

Thank you for raising this concern about the SUEWS modelling. We agree with your comment and have modified the forcing height to an appropriate level. Our initial idea was to use the same measurements for all the models to get a full model comparison without any biases concerning the forcing data. We now scaled the observed 2 m air temperature using a lapse rate of $6.5^{\circ}\text{C}/\text{km}$ to height of the wind and radiation measurements (35 m) and the 2 m air temperature is simulated within SUEWS and used to calculate photosynthesis and respiration, since they strongly depend on the local conditions. The text in the manuscript (Section 2.3) was updated to include this information (see our first response above). This change had a minimal impact on the results and on the conclusions. Below you can find two figures comparing the daily aggregated GPP and Reco simulations of the original manuscript with the updated model outputs for the trees and the lawns of our study areas. We also provide in the attachment all the updated figures and tables of the manuscript using the new SUEWS outputs.

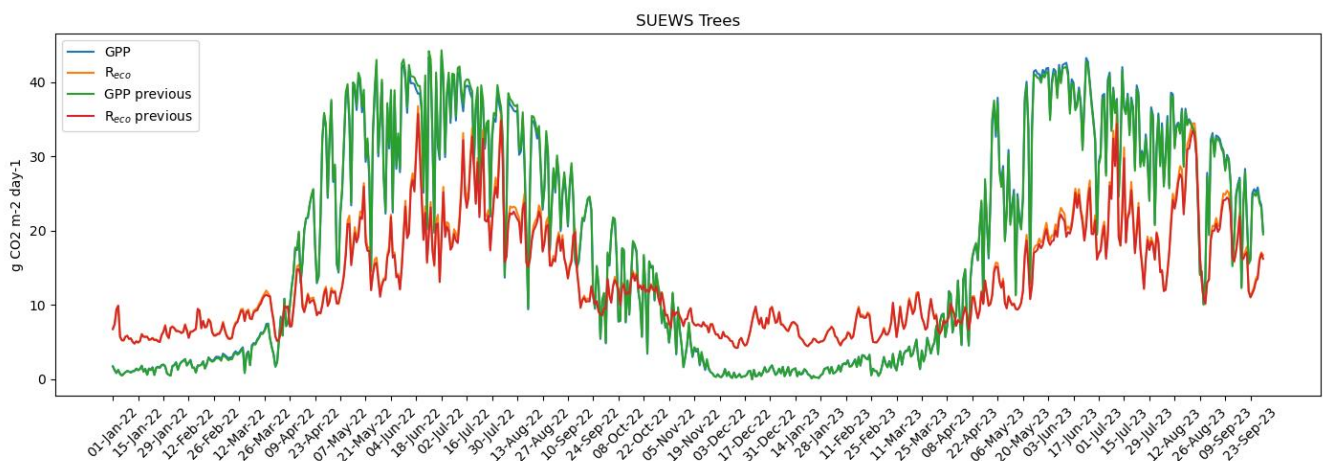


Fig. 1. GPP and Respiration of trees modelled with SUEWS, with previously used temperature and the updated version.

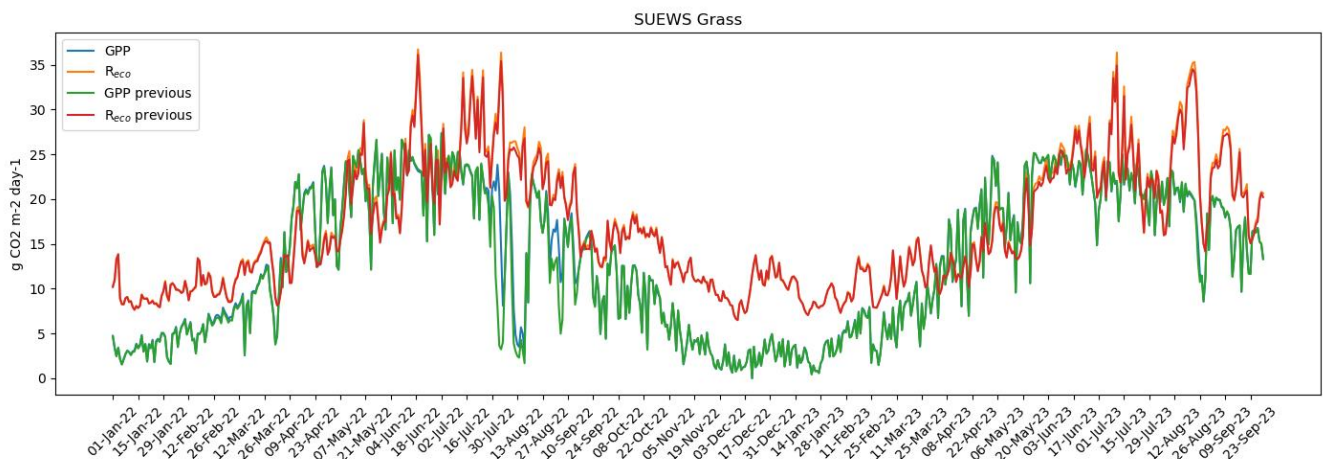


Fig. 2. GPP and Respiration of grass modelled with SUEWS, with previously used temperature and the updated version.

2. LAI Configuration

- Issue: Figure A1a shows modelled LAI plateau suggesting maximum LAI not properly adjusted
- Need: Clarification or correction of LAI parameterization

We thank the reviewer for this comment regarding the modelled LAI in SUEWS. The idea in the manuscript was not to adjust the model run to the local conditions but rather run SUEWS in as default mode as possible. LAI values often reach the plateau in SUEWS simulations, but actually in our case the maximum LAI is only met in a few days/week after the LAI growth. Also, we see from the comparisons that the maxima LAI values from SUEWS are in the correct order of magnitude. We did however modify the growing degree days (GDD) and senescence degree days (SDD) parameters to get more accurate spring leaf-on and autumn leaf-off (parameters provided in the Supplement). We believe that the model shows reasonable performance compared to the other models and measurements, and is comparable to previous SUEWS studies such as Omidvar et al., 2020. For clarification, we added few sentences to the SUEWS description (Section 2.3, see the text in our first response).

Omidvar, H., Sun, T., Grimmond, S., Bilesbach, D., Black, A., Chen, J., Duan, Z., Gao, Z., Iwata, H., and McFadden, J. P.: Surface Urban Energy and Water Balance Scheme (v2020a) in vegetated areas: parameter derivation and performance evaluation using FLUXNET2015 dataset, *Geosci. Model Dev.*, 15, 3041–3078, <https://doi.org/10.5194/gmd-15-3041-2022>, 2022.

Technical Improvements Needed:

1. Figures and Tables

- Figure 1: Enhance map label readability

We have increased the legend fonts and some symbol sizes and colors. The new image is attached.

- Figure 2b: Correct caption misrepresenting Reco measurements

We have revised the caption text to be clearer and changed the symbol colour and size for Reco to enhance the figure readability (new figure attached). The new caption text for Fig. 2b is:

“(b) Average and standard deviation of the measured soil respiration (R_{soil}), measured lawn ecosystem respiration (R_{eco}) (sunny and shaded locations in different colour) and daily average air and soil temperatures where the shading refers to the standard deviation of the seven soil sensors.”

- Table 2: Include temporal aggregation methods

The Table 2 was updated with timestep and temporal aggregation methods. The updated table is attached.

2. Other presentation improvements

- Standardise CO₂ flux units throughout paper

Following the Referee's suggestion, we have kept CO₂ flux units uniform across the manuscript ($\mu\text{mol m}^{-2} \text{s}^{-1}$) except for the annual totals (Fig. 5) where the units were converted to $\text{kg m}^{-2} \text{a}^{-1}$ to facilitate the comparison with relevant literature.

- Define abbreviations (LSWI, EVI) at first use

EVI and LSWI are defined in the first use in Line 295 (Section 2.3.4):

“GPP is a light-dependent term using remote sensing vegetation indices, including the Enhanced Vegetation Index (EVI) and Land Surface Water Index (LSWI), combined with shortwave solar radiation to estimate the carbon uptake from photosynthesis.”

- Include model parameter sets in data availability section

We have added the model parameter sets, as provided in the Supplement, in the metadata description of the datasets in Zenodo <https://doi.org/10.5281/zenodo.13222637>

We also made this clear in the Data availability section:

“ iv. modelled CO₂ fluxes and model parameter sets, are available in Zenodo repository under Creative Commons Licence CC-BY-4.0 (<https://doi.org/10.5281/zenodo.13222637>)”